Southern Ocean Sea Spray Emissions Parameter Estimation with an Observer

Dana McGuffin*[1], Erik Ydstie[1] and Peter Adams[2]

[1]Department of Chemical Engineering, Carnegie Mellon University, Pittsburgh, PA 15213
[2]Department of Civil & Environmental Engineering, Carnegie Mellon University, Pittsburgh, PA 15213

Abstract

An asymptotic observer is applied to estimate sea spray emissions over the Southern Ocean band. Estimations were derived from a global 3D chemical transport model and microphysical package adapted with an observer using satellite observations of aerosol optical depth. We designed the observer using a control Lyapunov function and tuned it to produce optimal performance. Results from the observer using a tuning parameter of six hours agrees with previous work, which estimated sea spray emissions based on sea surface temperature.

Keywords

Observer, Lyapunov, Parameter estimation, Remote sensing, Sea spray

Literature Review

The atmosphere contains a mixture of gaseous and particulate pollutants generated by a wide range of sources. Airborne particles, composed of solid and liquid phases, known as "aerosols" tend to scatter/reflect radiation causing a net effect of global cooling while greenhouse gases absorb radiation causing a net effect of global warming. Aerosols also impact cloud physics by changing their optical properties and formation of precipitation, which is collectively known as the aerosol indirect effect. Particles that contribute to the aerosol indirect effect are known as cloud condensation nuclei (CCN). The CCN enable cloud droplets to form as water condenses onto pre-existing CCN particles depending on the composition, concentration, and size of the aerosol (Seinfeld and Pandis, 2006). The balance between overall aerosol and greenhouse gas effects is poorly understood at present and represents one of the major uncertainties in predicting climate into the next decades. Models have been developed to estimate CCN concentration distributions and their effect on radiative forcing with widely varying results and degrees of accuracy (Cubasch et al., 2013; Wang et al., 2011) because of the multi-scale nature of the dynamics and sparsity of CCN-related measurements.

In a remote marine environment, the most significant source of aerosols is natural emissions resulting in a composition profile (in order of decreasing contribution) of sea-salt, non-sea-salt sulfate, mineral dust, and nitrate; however, the concentration of the last three compounds is collectively at least an order of magnitude lower than the concentration of sea-salt (Fitzgerald, 1991). Therefore, sea-salt is the most significant source of remote marine aerosols generated by sea spray. Sea Salt Aerosols (SSA) are mostly formed from breaking waves that generate bursting bubbles to form "film and jet drops" followed by wave tearing at high wind speeds resulting in "spume drops" (Lewis and Schwartz, 2004). These emissions have been studied under different meteorological conditions to determine parameterizations and methodologies describing the production of SSA based on laboratory experiments and field measurements (Monahan et al., 1986; Mårtensson et al., 2003; Gong, 2003; Clarke et al., 2006; O'Dowd et al., 2008; Sofiev et al., 2011; Jaeglé et al., 2011). In the past, SSA parameterizations have been directly determined based on measurements of sea spray and often validated with optical depth data (Witek et al., 2016). However, there are difficulties in using SSA field measurements to determine a general aerosol flux source function since the measurements widely vary with their conditions.

There are large; long-term; and rapidly growing data sets generated by satellite observations that indirectly relate to aerosol burden and SSA, which allow extrapolation of the parametrization to varying conditions. Process control is often used to determine representative measurements for accu-

*To whom all correspondence should be addressed *dmcguffi@andrew.cmu.edu*

rate estimations in addition to stabilizing systems with indirect measurements. Therefore, it is desirable to use process control theory as a framework for estimating parameters that describe atmospheric dynamics. Typical parameter estimation approaches involve a least-squares optimization routine in which knowledge of uncertainty in both model predictions and observations is vital (Jacob, 2007). A nonlinear feedback observer, the approach taken here, deviates from the more classical techniques such as Kalman Filtering by formulating an estimation scheme that is based on the exact system dynamics instead of a local linear approximation and its inherent uncertainty (Todling, 2000), which can be difficult to determine.

Methods

The Southern Ocean band just North of Antarctica (42°S – 82 °S) is a remote marine area in which aerosol optical depth is dominated by the contribution from SSA, and it reaches across the globe East to West so that longitudinal boundary conditions are not relevant. As a proof-of-concept, this paper focuses on designing an observer for estimating SSA emissions in the Southern Ocean band using a 3-D chemical transport model.

SSA Emissions Flux

The sea spray emissions generate a number flux of SSA (F_N),

$$\frac{dF_N}{dlogD_p} = 3.84 \cdot 10^{-6} U_{10}^{3.41} \sum_{i=1}^{3} \sum_{j=0}^{5} \beta_{i,j} D_p^j \quad . \tag{1}$$

This expression was determined by Clarke et al. based on field measurements at the University of Hawaii Bellows Air Force Station as a function of wind speed at a 10 m-altitude (U_{10}), emitted dry particle diameter (D_p), and the empirical constants ($\beta_{i,j}$) (Clarke et al., 2006). The *i* index corresponds to the size of SSA emitted while the *j* index represents the term of a fifth-order polynomial fit. It is apparent from (1) that wind speed takes on a significant role in determining SSA emissions, which is physically interpreted as a measure on the fraction of breaking waves at any point in time. However, this functional form of SSA emissions does not capture the complete physical phenomena that generates SSA since it is based on one simplified formation mechanism; conditions besides wind speed have previously shown to affect SSA flux, such as sea surface temperature (Jaeglé et al., 2011).

MODIS Observation Dataset

Acquiring global SSA concentration profiles with high temporal resolution to better estimate sea spray emissions is not a realistic task, so instead we will utilize a global dataset of aerosol optical depth (AOD). NASA's Terra satellite contains a suite of instruments to measure data related to climate change including a MODerate Resolution Imaging Spectroradiometer (MODIS). MODIS measures the Earth's reflected radiance in spectral bands between 470 and 2130 nm, which is used with cloud coverage to retrieve AOD at 550 nm. The satellite is in a sun synchronous orbit so that it makes one revolution around the Earth over the course of about 99 minutes and retrieves near global coverage daily. During each revolution, retrieved AOD is discretized into 5 minute intervals covering a 2330 km-long square with a pixel for every 9 km^2.

After Terra has made it around the entire globe each day, it has acquired enough data to cover the Southern Ocean band. Therefore, we will average data in this region throughout a day to determine a daily average AOD of the Southern Ocean. Although AOD has a complex dependence on physical properties of aerosol burden, we will assume a SSA profile with uniform light extinction and near-ambient marine conditions of 80% relative humidity. The proposed observer computes AOD from modelled dry aerosol mass burden (M_t) with a mass extinction coefficient (α_{ext}), optical adjustment for water uptake at a relative humidity (***f(RH)***), and surface area (*A*):

$$AOD = \frac{\alpha_{ext} f(RH)}{A} M_t \, . \tag{2}$$

The surface area, *A*, of the Southern Ocean band is near 30 million square-miles. The mass extinction coefficient is near 2.03 m^2/g for dry SSA (Hand and Malm, 2007), and the adjustment of sea-salt light extinction at 80% RH from dry conditions is approximately 2 (Carrico et al., 1998).

Chemical Transport and Microphysical Model

The framework for determining M_t and its rate of change is a global chemical transport model, GEOS-Chem, combined with the TwO-Moment Aerosol Sectional (TOMAS) microphysics package. GEOS-Chem is a 3-D, global model with inputs from the Goddard Earth Observing System (GEOS) for meteorological fields (Bey et al., 2001). GEOS-Chem v9-02 with a resolution of 4°x5°and 47 vertical layers spanning an altitude of approximately 80 km was used with GEOS Version 5 meteorology. TOMAS was used for the size-resolved aerosol species with respect to mass, which

keeps track of 10 logarithmically-spaced bins that correspond to diameters between 10 nm and 1 μm in addition to two bins for supermicron aerosols. The model uses an operator splitting technique to determine the overall mass balance,

$$\begin{aligned}&\frac{\partial m_{s,p,t}}{\partial t} = (\frac{\partial m_{s,p,t}}{\partial t})_{adv} + (\frac{\partial m_{s,p,t}}{\partial t})_{diff} + ... \\ &+(\frac{\partial m_{s,p,t}}{\partial t})_{dep} + R_{s,p,t} + E_{s,p,t} + (\frac{\partial m_{s,p,t}}{\partial t})_{coag} + ... \\ &+(\frac{\partial m_{s,p,t}}{\partial t})_{nuc} + (\frac{\partial m_{s,p,t}}{\partial t})_{cond} \quad ,\end{aligned} \tag{3}$$

for all species *s* in each grid box *p* at every time-step *t*, which encompasses several sinks and sources: advection, diffusion, wet and dry deposition, chemical production (*R*), emission sources (*E*), coagulation, nucleation, condensation/evaporation. The last three mechanisms of production in Equation (3) are specific to aerosol-species calculated from the TOMAS package, so they do not contribute to the mass balance for gas-phase and non-aerosol species. The net production is calculated by combining the generation/consumption from each term based on a forward explicit Euler integration. An example output of GEOS-Chem TOMAS is shown in Figure 1 for the average concentration of sea-salt aerosol throughout October 2010.

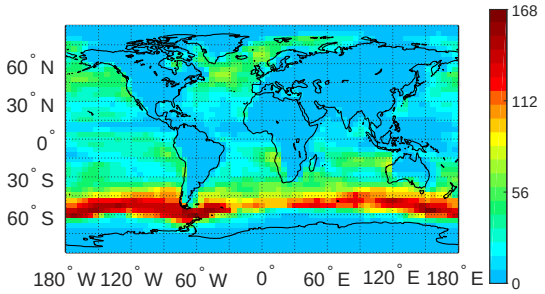

Figure 1. Modelled average sea-salt aerosol concentration ($\mu m/m^3$) for October 2010

Observer Design

From the global and complete atmospheric speciation, the subset that either make up dry aerosol or are affected by sea spray over the Southern Ocean band were taken into account to form a reduced-state space, which includes six components each resolved into 12 size bins: number of particles, sulfate, sea-salt, elemental carbon, organic carbon, dust. The reduced-state space considered here is a cumulative dry aerosol mass and aerosol number over this region (M_t and N_t) along with the unknown sea spray scaling factor (θ_t), which has a nominal value of one for a perfect model. To reconstruct the mass balance equation with θ_t, the net production of aerosol dry mass and number (F and F_n) is found for a time interval of Δt by combining all terms in Equation (3) and taking out the controlling factor: sea-salt mass and number emissions from the total emissions term (*E*). After integrating Equation (1) over the aerosol size range, the total sea spray mass and number emissions ($E_{SSA,\,t}$ and $E_{nSSA,\,t}$) is scaled by θ_t and added to the mass and number production rate. The scaling factor is set to one in the original model, but takes on a fraction greater or less than one for either a positive or negative model bias. The discrete-time system is

$$\begin{aligned}M_t &= M_{t-1} + \Big(F_{t-1} + \theta_{t-1}E_{SSA,\,t-1})\Big)\Delta t \\ N_t &= N_{t-1} + \Big(F_{n,\,t-1} + \theta_{t-1}E_{nSSA,\,t-1}\Big)\Delta t \\ y_t &= \tfrac{4.06}{A}M_t\end{aligned} \tag{4}$$

with a linear relationship for determining AOD (y_t) based on the RH-adjusted mass extinction coefficient ($\alpha_{ext} \cdot f(RH)$) and surface area of the Southern Ocean band (*A*). The observer is implemented in the model to estimate the scaling factor $\hat{\theta}_t$ so that the estimated state-space and the estimated output are represented as $\hat{M}_t$, $\hat{N}_t$, and $\hat{y}_t$ respectively. The parameter estimate $\hat{\theta}_t$ is found by determining a Control Lyapunov Function (CLF), $V(\hat{y})$, that describes the system (4) and satisfies three conditions,

$$V(\hat{y}) = 0 \quad for\ \hat{y} = y^m \tag{5}$$

$$V(\hat{y}) > 0 \quad \forall\ \hat{y} \neq y^m \tag{6}$$

$$\frac{dV}{dt} = \frac{\partial V}{\partial(\hat{y} - y^m)}\Big(\frac{d\hat{y}}{dt} - \frac{dy^m}{dt}\Big) \leq 0 \quad \forall\ \hat{y}, \tag{7}$$

so that the system achieves stability and convergence to a set of observations y^m (Khalil, 2002). The method adopted to determine a valid CLF is based on the quadratic function

$$V(\hat{y}_t) = \frac{1}{2}\Big(\hat{y}_t - y_t^m\Big)^2 \tag{8}$$

since *V* takes on its minimum value at y^m and is always positive satisfying constraints (5) and (6), respectively. Then, a negative quadratic $\frac{dV}{dt}$ satisfies Equation (7) by equating the output error rate of change to the error scaled by a negative proportionality constant. This approach results in proportional control of *V* by solving

$$\frac{\partial \hat{y}_t}{\partial \hat{M}_t}\Big(F_t + \hat{\theta}_t E_{SSA,\,t}\Big) - \frac{dy_t^m}{dt} = -C\Big(\hat{y}_t - y_t^m\Big) \tag{9}$$

for $\hat{\theta}_t$ where *C* is a positive gain constant. Replacing the proportional gain *C* with $1/\tau$ where τ represents a measure

of the observer convergence time gives

$$\hat{\theta}_t = E^{-1}_{SSA,\,t-1}\left[\frac{A}{\alpha_{ext} f(RH)}\frac{dy^m_t}{dt} - \frac{A}{\tau\alpha_{ext} f(RH)}\left(\hat{y}_{t-1} - y^m_t\right) - \frac{\Delta t}{\tau}\left(F_{t-1} + \hat{\theta}_{t-1}E_{SSA,\,t-1}\right) - F_t\right]. \tag{10}$$

Results & Discussion

The observer update of $\hat{\theta}_t$ was implemented into GEOS-Chem+TOMAS throughout a 15-month simulation starting October 2009, and the first three months were discarded as model "spin-up" to remove artificial effects from uncertain initial conditions. Instead of analyzing the observer start-up performance, we observe its ability to estimate satellite AOD.

Proof-of-Concept

The first set of results represents a "proof-of-concept" simulation since a constant value of 0.53, two times the modelled GEOS-Chem+TOMAS AOD, was implemented as a fictitious annual AOD to see how well the observer can recreate a given profile. Figure 2 shows these results using four differently tuned observers. As τ decreases, the AOD estimate gets closer to the set point of 0.53 such that if τ is greater than 144 hours, the observer has negligible effects on the modelled AOD and if τ is set to 1 hour, the observer oscillates.

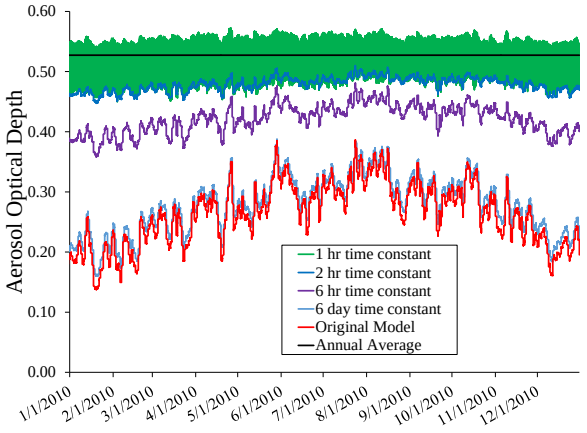

Figure 2. Estimated AOD proof-of-concept

The observer with τ equal to 6 hours results in estimated AOD with an annual profile similar to the original model dynamics, but scaled so that it is closer to the set point. The best performance appears with τ equal to 2 hours since it balances the tradeoff between oscillatory behavior and not replicating the observation dynamics. Average marine SSA residence time is on the order of hours (Gong et al., 2002), so a τ of 6 hours may be too long to capture the SSA dynamics whereas a τ of 2 hours leaves enough time for the estimated AOD to converge to the observed AOD before SSA are removed through the many aerosol sinks.

Observer Implemented with Satellite Observations

The same strategy was applied to the MODIS observations of daily average AOD, and the resulting estimate of AOD is shown in Figure 3 for τ less than the average SSA residence time. The estimations using actual satellite data with a 1 hour, 2 hour, and 6 hour τ qualitatively replicate the proof-of-concept results giving a normalized root mean square error of 41%, 60%, and 141% respectively.

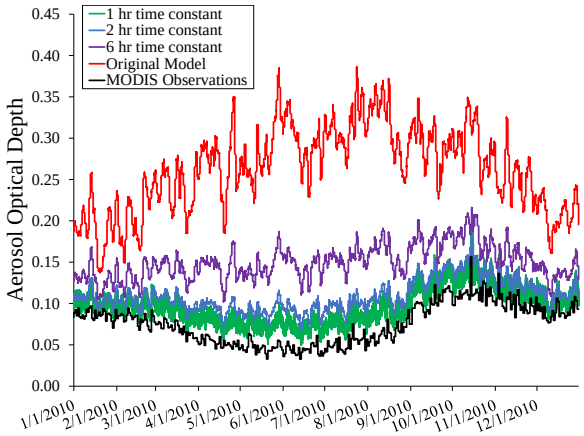

Figure 3. Estimated AOD from MODIS data

There is a larger offset between the set point and estimate for the 1 hour observer March through August indicating a seasonal variation that is not captured by the observer. The offset could originate from dynamics not captured by MODIS observations or in the modelled aerosol burden.

Scaling Factor

The estimated scaling factor gives intuition into the physical phenomena that the observer is applying to sea spray. Figure 4 shows the annual and daily dynamics of $\hat{\theta}$ from the 2 hour and 6 hour observers described above compared with previous corrections due to sea surface temperature (*SST*) that Jaeglé et al. estimated as a fifth-order polynomial in *SST* (Jaeglé et al., 2011).The annual $\hat{\theta}$ is 0.41, 0.46, and 0.60 for the 1 hour, 2 hour, and 6 hour time constants, respectively. Jaeglé corrections based on the modelled monthly Southern Ocean mean *SST* approximately line up with the 6 hour observer. Therefore, a larger portion of the corrections observed here seem to be influenced by temperature effects on sea spray flux. The 2 hour observer results in an annual $\hat{\theta}$ relative standard deviation of 24% while the observations y^m vary 32% from their annual average.

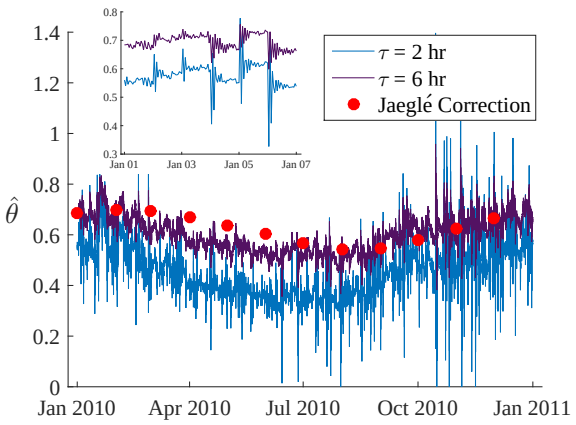

Figure 4. Estimated scaling factor from MODIS data with an inset of the daily response.

Conclusions

The proposed estimation scheme of a sea spray scaling factor based on a squared-error CLF applied to a nonlinear observer can attain a constant, annual AOD as well as a dynamic profile from satellite observations. The estimated output converges to the observations with an offset if τ is 6 hours or less while there is no significant difference between the model and the estimation if $\tau \geq 144$ hours. Additionally, the AOD estimate oscillates when τ is set to 1 hour because the control action over-corrects at each time step.

The 2 hour observer, which results in an annual mean sea spray scaling factor of 0.41, remains the best estimate of MODIS daily AOD observations since it is slow enough to inhibit oscillatory action and fast enough to follow the observation profile. The 1 hour observer results in an annual $\hat{\theta}$ with a relative standard deviation of 93%. This variance decreases for increasing τ, yet the profile does not precisely replicate the observation dynamics if $\tau \geq 6$ hours. Despite the simplifications in estimating AOD and sparsity of observations due to cloudy conditions and inadequate retrieval, estimations of AOD agree with previous work completely independent of optical measurements.

References

Bey, I., Jacob, D. J., Yantosca, R. M., Logan, J. A., Field, B. D., Fiore, A. M., Li, Q.-B., Liu, H.-Y., Mickley, L. J., and Schultz, M. G. (2001). Global Modeling of Tropospheric Chemistry with Assimilated Meteorology: Model Description and Evaluation. *Journal of Geophysical Research*, 106:73–95.

Carrico, C. M., Rood, M. J., and Ogren, J. a. (1998). Aerosol light scattering properties at Cape Grim, Tasmania, during the First Aerosol Characterization Experiment (ACE 1). *Journal of Geophysical Research*, 103(D13):16565.

Clarke, A. D., Owens, S. R., and Zhou, J. (2006). An ultrafine sea-salt flux from breaking waves: Implications for cloud condensation nuclei in the remote marine atmosphere. *Journal of Geophysical Research Atmospheres*, 111(6):1–14.

Cubasch, U. D., Chen, D., Facchini, M., Frame, D., Mahowald, N., and Winther, J. G. (2013). *Climate Change 2013: The Physical Science Basis. Contribution of Working Group I to the Fifth Assessment Report of the Intergovernmental Panel on Climate Change [Stocker, T.F., D. Qin, G.-K. Plattner, M. Tignor, S.K. Allen, J. Boschung, A. Nauels, Y. Xia, V. Bex and P.M. Midgley (eds.)]*. Cambridge University Press.

Fitzgerald, J. W. (1991). Marine aerosols: A review. *Atmospheric Environment. Part A. General Topics*, 25(3-4):533–545.

Gong, S. L. (2003). A parameterization of sea-salt aerosol source function for sub- and super-micron particles. *Global Biogeochemical Cycles*, 17(4):1–7.

Gong, S. L., Barrie, L. A., and Lazare, M. (2002). Canadian Aerosol Module (CAM): A size-segregated simulation of atmospheric aerosol processes for climate and air quality models 2. Global sea-salt aerosol and its budgets. *Journal of Geophysical Research Atmospheres*, 107(24):1–14.

Hand, J. L. and Malm, W. C. (2007). Review of aerosol mass scattering efficiencies from ground-based measurements since 1990. *Journal of Geophysical Research Atmospheres*, 112(16).

Jacob, D. (2007). Inverse modeling techniques. In Visconti, G., Carlo, P. D., Brune, W. H., and Schoeberl, M., editors, *Observing Systems for Atmospheric Composition*, chapter 17. Springer.

Jaeglé, L., Quinn, P. K., Bates, T. S., Alexander, B., and Lin, J.-T. (2011). Global distribution of sea salt aerosols: new constraints from in situ and remote sensing observations. *Atmospheric Chemistry and Physics*, 11:3137–3157.

Khalil, H. (2002). *Nonlinear Systems*. Prentice Hall, 3rd edition.

Lewis, E. R. and Schwartz, S. E. (2004). *Sea Salt Aerosol Production: Mechanisms, Methods, Measurements and Models - A Critical Review*. American Geophysical Union.

Mårtensson, E. M., Nilsson, E. D., de Leeuw, G., Cohen, L. H., and Hansson, H.-C. (2003). Laboratory simulations and parameterization of the primary marine aerosol production. *Journal of Geophysical Research*, 108:1–12.

Monahan, E. C., Spiel, D. E., and Davidson, K. L. (1986). A model of marine aerosol generation via whitecaps and wave disruption. In Monahan, Edward C. Niocaill, G. M., editor, *Oceanic Whitecaps And Their Role in Air-Sea Exchange Processes*, pages 167–174. D. Reidel Publishing.

O'Dowd, C. D., Langmann, B., Varghese, S., Scannell, C., Ceburnis, D., and Facchini, M. C. (2008). A combined organic-inorganic sea-spray source function. *Geophysical Research Letters*, 35(1):1–5.

Seinfeld, J. H. and Pandis, S. N. (2006). *Atmospheric Chemistry and Physics From Air Pollution to Climate Change*. John Wiley & Sons, Inc., 2nd edition.

Sofiev, M., Soares, J., Prank, M., De Leeuw, G., and Kukkonen, J. (2011). A regional-to-global model of emission and transport of sea salt particles in the atmosphere. *Journal of Geophysical Research Atmospheres*, 116(21).

Todling, R. (2000). Estimation theory and atmospheric data assimilation. In Kasibhatla, P., Heimann, M., Rayner, P., Mahowald, N., Prinn, R., and Hartley, D., editors, *Inverse Methods in Global Biogeochemical Cycles*. American Geophysical Union.

Wang, M., Ghan, S., Ovchinnikov, M., Liu, X., Easter, R., Kassianov, E., Qian, Y., Morrison, H., and Liu, X. (2011). Aerosol Indirect Effects in a Multi-Scale Aerosol- Climate Model PNNL-MMF Aerosol indirect effects in a multi-scale aerosol-climate model PNNL-MMF. *Atmospheric Chemistry and Physics*, 11(11):5431–5455.

Witek, M., Diner, D., and Garay, M. (2016). Satellite assessment of sea spray aerosol productivity: Southern Ocean case study. *Journal of Geophysical Research : Atmospheres*, 121(2):872–894.